Scots pine trees react to drought by increasing xylem and phloem conductivities

Natasa Kiorapostolou[1], J. Julio Camarero[2], Marco Carrer[1], Frank Sterck[3], Brigita Brigita[3], Gabriel Sangüesa-Barreda[4,2], Giai Petit[1]

[1]Dip. Territorio e Sistemi Agro-Forestali, Università di Padova, Viale dell'Università 16, 35020 Legnaro (PD), Italy

[2]Instituto Pirenaico de Ecologia (IPE-CSIC), Avda Montanana 1005, Zaragoza 50059, Spain

[3]Forest Ecology and Forest Management group, Wageningen University, 6700 AA, Wageningen, the Netherlands

[4]Depto. Ciencias Agroforestales, iuFOR-EiFAB, University of Valladolid, Campus Duques de Soria s/n, E-42004 Soria, Spain

* For correspondence: natasa.kiorapostolou@phd.unipd.it

Running head: Wood anatomy in drought-stressed Scots pines

Abstract

Drought limits the long-distance transport of water in the xylem due to the reduced leaf-to-soil water potential difference and possible embolism-related losses of conductance, and of sugars in the phloem due to the higher viscosity of the dehydrated sugary solution. This condition can have cascading effects in water and carbon fluxes that may ultimately cause tree death. We hypothesize that the maintenance of xylem and phloem conductances is fundamental for survival also under reduced resource availability, when trees may produce effective and low C cost anatomical adjustments in the xylem and phloem close to the treetop where most of the hydraulic resistance is concentrated.

We analyzed the treetop xylem and phloem anatomical characteristics in coexisting Scots pine trees symptomatic and non-symptomatic of drought-induced dieback. We selected the topmost 55 cm of the main stem and selected several sampling positions at different distances from the stem apex to test for differences in the axial patterns between the two groups of trees. We measured the annual ring area (*RA*), the tracheid hydraulic diameter (*Dh*) and cell wall thickness (*CWT*), the conductive phloem area (*PAcond*) and the average lumen diameter of the 20 largest phloem sieve cells (*Dph*).

Declining trees grew less than the non-declining ones, and despite the similar axial scaling of anatomical traits, had larger *Dh* and lower *CWT*. Moreover, declining trees had wider *Dph*.

Our results demonstrate that even under drought stress, maintenance of xylem and phloem efficiencies is of primary importance for survival, even if producing fewer larger tracheids may lead to a xylem more vulnerable to embolism formation.

Keywords: *Pinus sylvestris*, wood anatomy, forest dieback, tree mortality, hydraulic failure, phenotypic plasticity, xylem, phloem.

Introduction

Drought events and heat waves are increasing worldwide in frequency and intensity due to the effects of climate change (Dai 2013). The resulting soil water shortage and high evaporative demand impose serious limitations to leaf transpiration and C uptake, inducing challenging conditions for the survival of trees. Indeed, an increased frequency of forest dieback and tree mortality events has been reported worldwide in the last decades (Allen et al. 2015).

Tree survival is dependent on the maintenance of a positive C balance, i.e., the difference between C uptake through photosynthesis and C used for all the different physiological processes including growth and respiration. Maintenance respiration consumes approximately 50% of the total C fixed with photosynthesis (Waring et al. 1998). Other significant amounts of C (>20% of the total C fixed with photosynthesis) are transferred to the soil as root exudates and to the atmosphere as volatile organic compounds (VOCs) (Preece et al. 2018, Ameye et al. 2018).

Gas exchange mainly occurs through the stomata. While CO_2 diffuses from the atmosphere inside the mesophyll, where is fixed by photosynthesis, the water evaporating from the mesophyll cell walls diffuses to the atmosphere. The water lost with evapotranspiration needs to be replaced by water absorbed by roots and flowing along the xylem transport system to the leaves. According to the Darcy's law ($F=\Delta\Psi\times K$) (Tyree & Ewers 1991), the water flow (F) sustaining leaf transpiration is proportional to the difference of water potential between leaves and roots ($\Delta\Psi=\Psi_{LEAF}-\Psi_{SOIL}$) and to the total xylem conductance (K). K depends on the hydraulic contribution of every single xylem conduit constituting the water transport system. Since K cannot be promptly modified because xylem conduits are dead hollow cells, a reduction in $\Delta\Psi$ due to soil drought (i.e., lower Ψ_{SOIL}) can be

limiting for *F*, and therefore for gas exchange. If this situation persists until the tree depletes all the C reserves, decline and finally death by C starvation would occur.

Another major mechanism of canopy dieback and tree death implies widespread xylem embolism leading to plant desiccation by hydraulic failure (McDowell et al. 2008). The evaporation from cellular interstices in the leaf mesophyll cavities implies that water flows along the xylem at sub-atmospheric pressure and therefore in a metastable liquid phase (Cohesion Tension Theory: Dixon & Joly 1894). When water potential drops below a certain threshold, air bubbles can penetrate and expand into a xylem conduit, which becomes air-filled and no longer conductive (Cochard 2006). Vulnerability of conduits to embolism formation is variable and depends on different anatomical structures (e.g., pit size and number) (Tixier et al. 2014). In general, embolism resistance decreases with increasing conduit size (Hacke et al. 2006, Sperry et al. 2006), especially at the intraspecific level (Larter et al. 2017). Accordingly, the smallest xylem conduits along the roots-to-leaves hydraulic path are found at the stem apex (e.g., Petit et al. 2010), where the water potential is the lowest due to the proximity to the sites of evaporation (i.e., leaves) (Venturas et al. 2017). Below the apex, conduits increase progressively until the stem base according to a universal axial pattern across species, sizes, and environments (Anfodillo et al. 2013).

In parallel to water flowing upwards to the leaves along the xylem, the solution of sugars produced with photosynthesis flows along the phloem, where sieve elements increase in diameter from the stem apex to base similarly to the axial pattern of xylem conduits (Petit & Crivellaro 2014, Jyske & Hölttä 2015, Savage et al. 2017). The flow occurs under the positive pressure between the sites of sugar loading (leaves, with higher sugar concentration) and sink sites, where sugars are consumed (De Schepper et al. 2013). This drop of positive pressure is sustained by sugar loading at the leaf level. Consequently, sugar transport is dependent on C assimilation and thus on leaf transpiration (Hölttä et al. 2006). Under

drought, not only the reduced photosynthesis following stomatal closure can negatively affect the source-to-sink pressure difference and thus limit the transport of sugars, but also overall phloem hydraulic efficiency (i.e., conductance) can be further limited by the higher sap viscosity due to tissue dehydration (Sevanto 2014).

What mechanism is mostly involved in determining irreversible conditions and exposing trees to pathogens attacks and ultimately mortality has been the object of intense research in the last decade (McDowell et al. 2013, Gaylord et al. 2015). The most common case that has been reported in trees at significant stressful conditions preceding drought-induced mortality, is a high loss of conductance (>60%) due to widespread embolism formation (Adams et al. 2017). Moreover, this condition is often associated with a reduction in both primary and secondary growth (e.g., Weemstra et al. 2013, Camarero et al. 2015), implying limitations for the plant's carbon balance.

In this context, phenotypic adjustments of xylem and phloem anatomies would commonly be expected to occur, according to natural variability along environmental gradients, allowing trees to maintain functionality.

Several studies reported narrower xylem conduits in drier environments (e.g., Pfautsch et al. 2016, Martínez-Sancho et al. 2017), suggesting that a safer xylem against air seeding is necessary under higher xylem tensions. Furthermore, phloem sieve elements have been also reported to be narrower under drought, suggesting a stronger limitation to the long distance transport of sugars (Dannoura et al. 2018).

However, according to the most widely used sampling protocols the anatomical measurements are taken only at one single sampling position, i.e., either at the stem base or on branches of characteristic age (usually 2-3 years). Such methodological approaches substantially neglect that anatomical traits (e.g., xylem conduit diameter and phloem sieve cell diameter) vary axially with the distance from the stem/branch apex (Anfodillo et al.

2013). Therefore, plants with reduced growth rates and shorter statures (i.e., the typical features of plants growing in dry conditions) would be sampled at shorter distance from the apex, where xylem conduits and phloem sieve elements are smaller per se.

The overall picture of anatomical adjustments described above, conflicts with other analyses carried out according to different sampling approaches, accounting for the general and predictable axial design of the xylem and phloem architectures. Emerging evidence from such studies is showing that plants' responses to drought do not imply the production of smaller and safer conduits. That is, conduits increase with the distance from the apex at rates that are not influenced by environmental conditions, and the absolute conduit diameter was found to be either similar (Lechthaler et al. 2018, Kiorapostolou & Petit, 2018) or wider all along the longitudinal stem/branch axis in drier conditions (Petit et al. 2016, Kiorapostolou et al. 2018). Seemingly, phloem sieve elements and phloem area were reported to increase with the distance from the apex, with drought stimulating plants producing a more conductive phloem architecture (i.e., larger phloem area and larger sieve cells: Kiorapostolou & Petit 2018), likely maintaining the overall efficiency of sugar transport system (Sevanto 2014).

Tree must maintain a positive C balance to survive. Therefore, they need to compensate for potential limitations to C assimilation and sugar transport. A possible solution would be optimizing the C investment into the xylem and phloem architectures by reducing the allocation to new biomass (i.e., slower primary and secondary growth), while maintaining or even increasing the xylem and/or phloem conductance by producing larger conductive cells.

The aim of this study was to compare the xylem and phloem anatomy of the topmost part of the main stem (i.e., the hydraulic bottleneck) of coexisting Scots pine (*Pinus sylvestris* L.) trees symptomatic and non-symptomatic of drought-triggered dieback. The target population was already object of a retrospective dendro-anatomical analysis revealing that the

production of narrower conduits at 1.3 m started decades before evident signals of dieback such as needle loss and growth decline (Pellizzari et al. 2016). The null hypothesis was that symptomatic trees differ from non-symptomatic ones not only because they form narrower tracheids at the stem base (Pellizzari et al. 2016), but also because they produce larger tracheids at the stem apex in order to maintain the total hydraulic conductance with reduced C allocation to xylem biomass. Moreover, phloem anatomy of declining trees is expected to be characterized by a higher conductive area and wider sieve elements to guarantee an adequate efficiency of the long-distance transport of a more viscous phloem sap due to stronger drought-induced tissue dehydration.

Materials and methods

Plant material and study site

The study area is a Scots pine forest (0º 59' 18'' W, 40º 26' 32'' N, 1260-1289 m a.s.l.) located near Corbalán, Aragón (E. Spain), where many trees started defoliating and dying after the severe drought of 2012 (Supplementary Figure 1). Since then, mean mortality rates are approximately 12% yr^{-1} (J.J. Camarero, personal observation). Trees from this study area had been already subject of dendro-anatomical analyses by Camarero et al. (2015) and Pellizzari et al. (2016). In late April of 2017, we sampled the apical 55 cm of the stem axis (treetop) of three declining (with reduced foliage cover, on average less than 30% of total crown cover) and three non-declining Scots pine trees (crown cover > 90%) of similar height. For each sampled tree, measurements of diameter at breast height (1.3 m) and total height, and visual estimate of crown cover were performed in the field. Tree age was estimated by counting the number of rings in tree cores extracted at breast height (Table 1).

For each tree, we selected 4-15 sampling points along to topmost 55 cm of the stem. Sampling points were selected at approximately 1 cm from the base of each internode. Stem

segments were extracted at each sampling point, and then cut using a rotary microtome LEICA RM 2245 (Leica Biosystems, Nussloch, Germany) at 15-18 μm. Transverse micro-sections were stained with a solution of safranin and Astra Blue (1% and 0.5% in distilled water, respectively), and permanently fixed on glass slides with Eukitt (BiOptica, Milan, Italy). Images of micro-sections were acquired at 100x magnification, using a D-sight slide scanner (Menarini Group, Florence, Italy), and analysed with ROXAS (von Arx & Carrer 2014). The analysis was performed on a wedge of known angle (α, between 10 and 40 degrees) centred at the pith. Analysed images were first manually edited to outline the contour of the pith and of each xylem ring to allow a ring-based estimate of the xylem ring area of the image (*RA*), as well as of the conductive phloem area (*PAcond*). The average conduit hydraulic diameter ($Dh = \Sigma d^5/\Sigma d^4$, where d is the conduit diameter), and the cell wall thickness (*CWT*) were also measured. Then, each *RA* was up-scaled to the whole cross-section as $Y=Y'/\alpha \times 360$ (where Y is the up-scaled *RA*, Y' the *RA* of each ring, and α the wedge angle). Moreover, for each sampling point along the apical stem axis, the mean diameter of the 20 largest phloem sieve cells (*Dph*) of the most recent phloem ring (conductive phloem) was estimated after measuring their cell area and assuming cells to be circular. Similar analysis was used in (Kiorapostolou & Petit 2018).

Each ring-based anatomical trait was then related to the distance from the contemporary apex (i.e., the stem apex in that given year, *Dap*). When necessary, *Dap* was estimated on the basis of the average annual elongation rate between two successive discs ($\Delta H=\Delta NR/L$, where ΔNR is the difference in number of rings between two successive discs, and L is the distance between them). Therefore, the total number of samples per individual depended basically on its longitudinal growth rate.

Statistical analysis

We performed a comparative analysis of the scaling relationships between different traits (i.e., dependent variables: *RA, CWT, Dh, Dph*) against the distance from the apex (*Dap*) in declining and non-declining trees for the wood produced after the drought of 2012 (the last 5 annual rings of the sections). We used Standardized Major Axis (SMA) models and tested for possible differences on the elevation (*y*-intercept) and slope (exponent *b*) of the different scaling relationships (Warton et al. 2006, 2012). When necessary, variables were transformed in natural logarithm (log in R) to meet the assumptions of normality and homoscedasticity. All statistical analyses were performed using R version 3.4.2 (R Core Team, 2017).

Results

In both declining and non-declining trees, the annual allocation into xylem biomass followed an axial scaling relationship between the xylem ring area (*RA*) and the distance from the stem apex (*Dap*). The scaling exponent (i.e., the slope of the log-log relationship) was higher in declining compared to non-declining trees (Figure 1a; Table 2). However, declining trees grew significantly less than non-declining trees, as shown by their lower *y*-intercept in the relationship between *RA* and *Dap* (Figure 1a; Table 2), and by their lower stem elongation rates (mean ±SE = 2.37 ± 0.2 vs. 5.77 ±1.13 cm yr^{-1}).

The tracheid cell wall thickness (*CWT*) increased with *Dap* in the declining trees, whereas for non-declining trees the axial variation for the topmost 55 cm was negligible (Figure 1b; not significant slope). The declining trees had thinner cell walls closer to the stem apex, as shown by the significantly lower *y*-intercept in the relationship *CWT* vs. *Dap* (Figure 1b; Table 2).

Xylem tracheids revealed a clear axial pattern. The mean tracheid hydraulic diameter (*Dh*) increased with *Dap* following a power trajectory, with a scaling exponent (i.e., the slope

of the log-log relationship) not significantly different between declining and non-declining trees (Figures 1c; Table 2). However, declining trees produced wider tracheids (significantly higher *y*-intercept: Figure 1c; Table 2) than the non-declining trees.

We found that the cross sectional area of the total conductive phloem (*PAcond*) increased with *Dap* according to a similar power scaling in both declining and non-declining trees (Figure 2a; Table 2)

The average diameter of phloem sieve cells (*Dph*) increased with *Dap* following a power trajectory, with a scaling exponent not significantly different between declining and non-declining trees. However, declining trees produced wider sieve cells than the non-declining trees (significantly higher *y*-intercept: Figures 2b; Table 2).

Discussion

In this study, we performed xylem and phloem anatomical analyses at the treetop of coexisting Scots pine trees symptomatic and non-symptomatic of drought-induced decline of vigor. Our declining Scots pine trees revealed a long-term (>30 years) reduction in radial growth and tracheid diameter near the stem base (Pellizzari et al. 2016). On the contrary, our anatomical analyses of the most apical portion of the stem revealed that the same symptomatic trees did decrease the C investment into growth since tracheids were larger with thinner cell walls. Moreover, the treetops of declining trees had also larger phloem sieve cells compared to non-declining trees.

Our results coupled with those of Pellizzari et al. (2016) reveal that anatomical adjustments can differ between positions along the xylem and likely the phloem hydraulic paths. This opens a serious problem of interpretation of trees' long-term responses to drought and more generally to environmental variability, related to the number and positions of sampling points along the longitudinal axis of stem and branches and linked to the scientific

question. Lechthaler et al. (2018) already discussed that neglecting that anatomical traits (e.g., xylem conduit diameter) vary axially along a given ring according to the distance from the stem/branch apex, potentially leads to wrong interpretations of results. In fact, a single point sampling at the stem base (or at branches of fixed age) results in sampling positions closer to the apex (e.g., thus in narrower conduit diameters) for shorter trees (or branches with reduced elongation rates). Moreover, Prendin et al. (2018) recently suggested that trees can modify the axial design of the xylem architecture to maintain the total xylem conductance under reduced C availability. Conduits at the stem apex slightly increase to release the xylem's hydraulic bottleneck, while the overall lower investment of C into new xylem will result into narrower conduits closer to the stem base.

In this study, we compared the diameter variation of xylem tracheids and phloem sieve cells along the treetop. We found a clear convergence of both declining and non-declining trees towards the typical axial scaling of xylem conduit diameter vs. distance from the stem apex with exponent b~0.2. This provides further support to the hypothesis that selection favored this axial design irrespective of species, tree sizes, and environment (Anfodillo et al. 2006, Olson et al. 2014), likely because represents the best compromise of xylem hydraulic efficiency and safety al the lowest C cost (Mencuccini et al. 2007). Narrower and more cavitation-resistant conduits (Larter et al. 2017) are located at the stem apex, where xylem tensions are the highest (i.e., the lowest water potentials) (Venturas et al. 2017). Below, the progressively larger conduits would add a nearly negligible contribution to the total path hydraulic resistance, thus guaranteeing a good efficiency (i.e., total conductance) of the transport system (Petit and Anfodillo 2009).

Differences in the *y*-intercept of our assessed scaling relationships revealed that declining trees produced at their treetops narrower rings with larger tracheids of thinner walls, compared to non-declining trees. Declining trees produced narrower rings also near the

stem base, but associated with narrower tracheids (Pellizzari et al. 2016). With this xylem low C-cost configuration, the wider apical tracheids would theoretically compensate for the reduction in growth and hydraulic conductivity of narrower tracheids at the stem base (Prendin et al. 2018). However, larger apical tracheids had also thinner cell walls, suggesting that our symptomatic trees were likely more exposed to the risk of drought-induced embolism (Sperry et al. 2006), compared to non-symptomatic trees.

We found that both the total area of conductive phloem and the lumen diameter of sieve cells increased axially from the stem apex downwards. The increase in diameter of the phloem sieve cells for the first 55 cm from the apex was significant (b~0.3) (Table 2). Phloem architecture is characterized by conductive sieve cells that progressively increase in diameter from the stem apex towards the stem base (Petit & Crivellaro 2014, Jyske & Hölttä 2015, Savage et al. 2017, Kiorapostolou & Petit 2018), so that the treetop results to be the hydraulic bottleneck also for the long-distance sugar transport system (Ryan & Robert 2017, Savage et al. 2017). Interestingly, declining trees had similar phloem area, but with larger sieve cells, in agreement with the hypothesis that a higher phloem conductance is necessary to compensate for the negative effect of higher phloem sap viscosity on the efficiency of sugar transport under drought (Sevanto 2014).

The overall picture following our anatomical analyses and coupled with those of Pellizzari et al. (2016) showed that significant differences exist in the xylem and phloem anatomies of symptomatic and non-symptomatic trees showing different intensity of drought-induced dieback. Symptomatic trees were limited in the investment into new biomass and reduced radial growth and tracheid diameter near the stem base. However, they increased the conductivity of the stem apex by enlarging tracheids. This modification of xylem axial configuration would suggest a prioritization to the maintenance of a certain xylem conductive

efficiency, even if at the side cost of exposing to the highest tensions larger tracheids with thinner walls (i.e., more vulnerable to embolism formation).

Our analyses and interpretations re-evaluate the role of the xylem embolism resistance as no longer central in the prioritized processes of acclimation and adaptation to soil drought conditions. It can be argued that under reduced C availability, as under drought, producing narrower apical tracheids would decrease the total xylem conductance, with further negative effects on stomatal conductance and photosynthesis. Substantially, the tree reaction to drought unlikely produces a xylem more resistant to embolism, because this cannot be equally efficient (Gleason et al. 2016).

In conclusion, we demonstrated that the treetop is the region where low-cost but hydraulically effective anatomical modifications can be realized under drought stress, meristem impairment and shortage of C resources. Safeguarding the total xylem and phloem conductance seems a risk worth taking to increase the chances of survival, even though this may come at the cost of a higher vulnerability of embolism formation and the relative higher risk of death by hydraulic failure.

Conflict of interest

The authors declare that they have no conflict of interest.

Authors' contribution

GP, JJC and MC designed and GP coordinated the study. GSB, and JJC performed the sampling. BB and NK carried out the measurements. NK, JJC and FS performed the statistical analysis. NK wrote the manuscript with contributions by GP. All the authors contributed equally to the discussion and to the final version of this manuscript.

Acknowledgements

We are grateful to the colleagues from “Laboratorio de Sanidad Forestal (DGA)” at Mora de Rubielos, Aragón, Spain.

Funding

G. Sangüesa-Barreda was supported by a Juan de la Cierva-Formación grant from MINECO (FJCI 2016-30121). We acknowledge funding provided by the following Spanish projects. CGL2015-69186-C2-1-R, CGL2015-69186-C2-2-R and RTI2018-096884-B-C31. GP was supported by the Università degli Studi di Padova (DOR1877180/18).

References

Adams HD, Zeppel MJ, Anderegg WR, Hartmann H, Landhäusser SM, Tissue DT, ... Anderegg LD (2017) A multi-species synthesis of physiological mechanisms in drought-induced tree mortality. Nat Ecol Evol 1: 1285.

Allen CD, Breshears DD, McDowell NG (2015) An underestimation of global vulnerability to tree mortality and forest die-off from hotter drought in the Anthropocene. Ecosphere 6: 1-55.

Ameye M, Allmann S, Verwaeren J, Smagghe G, Haesaert G, Schuurink RC, Audenaert K (2018) Green leaf volatile production by plants: a meta-analysis. New Phytol 220: 666-683.

Anfodillo T, Carraro V, Carrer M, Fior C, Rossi S (2006) Convergent tapering of xylem conduits in different woody species. New Phytol., 169: 279-290.

Camarero JJ, Gazol A, Sangüesa-Barreda G, Oliva J, Vicente-Serrano SM (2015) To die or not to die: early warnings of tree dieback in response to a severe drought. J Ecol 103: 44-57.

Cochard H (2006) Cavitation in trees. Comptes Rendus Physique 7: 1018-1026.

Dai A (2013) Increasing drought under global warming in observations and models. Nature Climate Change 3: 52.

Dannoura M, Epron D, Desalme D, Massonnet C, Tsuji S, Plain C, ... Gérant D (2018) The impact of prolonged drought on phloem anatomy and phloem transport in young beech trees. Tree Physiol 39: 201-210.

De Schepper V, De Swaef T, Bauweraerts I, Steppe K (2013) Phloem transport: a review of mechanisms and controls. J Exp Bot 64: 4839-4850.

Dixon HH, Joly J (1894) On the ascent of sap. Philos Trans Roy Soc London, Ser B 186: 563-576.

Gaylord ML, Kolb TE, McDowell NG (2015) Mechanisms of piñon pine mortality after severe drought: a retrospective study of mature trees. Tree physiol 35: 806-816.

Gleason SM, Westoby M, Jansen S, Choat B, Hacke UG, Pratt RB, ... Cochard H (2016) Weak tradeoff between xylem safety and xylem-specific hydraulic efficiency across the world's woody plant species. New Phytol 209: 123-136.

Hacke UG, Sperry JS, Wheeler JK, Castro L (2006) Scaling of angiosperm xylem structure with safety and efficiency. Tree physiol 26: 689-701.

Hölttä T, Vesala T, Sevanto S, Perämäki M, Nikinmaa E (2006) Modeling xylem and phloem water flows in trees according to cohesion theory and Münch hypothesis. Trees 20: 67-78.

Jyske T, Hölttä T (2015) Comparison of phloem and xylem hydraulic architecture in *Picea abies* stems. New Phytol 205: 102-115.

Kiorapostolou N, Galiano-Pérez L, von Arx G, Gessler A, Petit G (2018) Structural and anatomical responses of *Pinus sylvestris* and *Tilia platyphyllos* seedlings exposed to water shortage. Trees 32: 1211-1218.

Kiorapostolou N, Petit G (2018) Similarities and differences in the balances between leaf, xylem and phloem structures in *Fraxinus ornus* along an environmental gradient. Tree Physiol 39: 234-242.

Larter M, Pfautsch S, Domec JC, Trueba S, Nagalingum N, Delzon S (2017) Aridity drove the evolution of extreme embolism resistance and the radiation of conifer genus *Callitris*. New Phytol 215: 97-112.

Lechthaler S, Turnbull TL, Gelmini Y, Pirotti F, Anfodillo T, Adams MA, Petit G (2018) A standardization method to disentangle environmental information from axial trends of xylem anatomical traits. Tree Physiol 39: 495-502.

Martínez-Sancho E, Dorado-Liñán I, Hacke UG, Seidel H, Menzel A (2017) Contrasting hydraulic architectures of Scots pine and sessile oak at their southernmost distribution limits. Front Plant Sci 8: 598.

McDowell N, Pockman WT, Allen CD, Breshears DD, Cobb N, Kolb T, ... Yepez EA (2008) Mechanisms of plant survival and mortality during drought: why do some plants survive while others succumb to drought? New Phytol 178: 719-739.

McDowell NG, Fisher RA, Xu C, Domec JC, Hölttä T, Mackay DS, ... Limousin JM (2013) Evaluating theories of drought-induced vegetation mortality using a multimodel–experiment framework. New Phytol 200: 304-321.

Mencuccini M, Hölttä T, Petit G, Magnani F (2007) Sanio's laws revisited. Size-dependent changes in the xylem architecture of trees. Ecol Lett 10: 1084-1093.

Olson ME, Anfodillo T, Rosell JA, Petit G, Crivellaro A, Isnard S, León-Gómez C, Alvarado-Cárdenas LO, Castorena M (2014) Universal hydraulics of the flowering plants: vessel diameter scales with stem length across angiosperm lineages, habits and climates. Ecol Lett. 17: 988-997.

Pellizzari E, Camarero JJ, Gazol A, Sangüesa-Barreda G, Carrer M (2016) Wood anatomy and carbon-isotope discrimination support long-term hydraulic deterioration as a major cause of drought-induced dieback. Global change Biol 22: 2125-2137.

Petit G, Anfodillo T, De Zan C (2009) Degree of tapering of xylem conduits in stems and roots of small *Pinus cembra* and *Larix decidua* trees. Botany 87: 501-508.

Petit G, Anfodillo T (2009) Plant physiology in theory and practice: an analysis of the WBE model for vascular plants. *J Theor Biol 259*: 1-4.

Petit G, Crivellaro A (2014) Comparative axial widening of phloem and xylem conduits in small woody plants. Trees 28: 915-921.

Petit G, Pfautsch S, Anfodillo T, Adams MA (2010) The challenge of tree height in *Eucalyptus regnans*: when xylem tapering overcomes hydraulic resistance. New Phytol 187: 1146-1153.

Petit G, Savi T, Consolini M, Anfodillo T, Nardini A (2016) Interplay of growth rate and xylem plasticity for optimal coordination of carbon and hydraulic economies in *Fraxinus ornus* trees. Tree Physiol 36: 1310-1319.

Pfautsch S, Harbusch M, Wesolowski A, Smith R, Macfarlane C, Tjoelker MG, ... Adams MA (2016) Climate determines vascular traits in the ecologically diverse genus *Eucalyptus*. Ecol Lett 19: 240-248.

Preece C, Farré-Armengol G, Llusià J, Peñuelas J (2018) Thirsty tree roots exude more carbon. Tree Physiol 38: 690-695.

Prendin AL, Mayr S, Beikircher B, von Arx G, Petit G (2018) Xylem anatomical adjustments prioritize hydraulic efficiency over safety as Norway spruce trees grow taller. Tree Physiol 38: 1088-1097.

R Development Core Team (2017) R: A language and environment for statistical computing. R Foundation for Statistical Computing, Vienna, Austria. URL https://www.R-project.org/

Ryan MG, Robert EM (2017) Zero-calorie sugar delivery to roots. Nature plants 3: 922.

Savage JA, Beecher SD, Clerx L, Gersony JT, Knoblauch J, Losada JM, ... Holbrook NM (2017) Maintenance of carbohydrate transport in tall trees. Nature plants 3: 965.

Sevanto S (2014) Phloem transport and drought. J Exp Bot 65: 1751-1759.

Sperry JS, Hacke UG, Pittermann J (2006) Size and function in conifer tracheids and angiosperm vessels. Am J Bot 93: 1490-1500.

Tixier A, Herbette S, Jansen S, Capron M, Tordjeman P, Cochard H, Badel E (2014) Modelling the mechanical behaviour of pit membranes in bordered pits with respect to cavitation resistance in angiosperms. An Bot 114: 325-334.

Tyree MT, Ewers FW (1991) The hydraulic architecture of trees and other woody plants. New Phytol 119: 345-360.

Venturas MD, Sperry JS, Hacke UG (2017) Plant xylem hydraulics: what we understand, current research, and future challenges. J Integ Plant Biol 59: 356-389.

Von Arx G, Carrer M (2014) ROXAS–A new tool to build centuries-long tracheid-lumen chronologies in conifers. Dendrochronologia 32: 290-293.

Waring RH, Landsberg JJ, Williams M (1998) Net primary production of forests: a constant fraction of gross primary production? Tree physiol 18: 129-134.

Warton DI, Wright IJ, Falster DS, Westoby M (2006) Bivariate line-fitting methods for allometry. Biol Reviews 81: 259-291.

Warton DI, Duursma RA, Falster DS, Taskinen S (2012) smatr 3–an R package for estimation and inference about allometric lines. Methods Ecology Evol 3: 257-259.

Weemstra M, Eilmann B, Sass-Klaassen UG, Sterck FJ (2013) Summer droughts limit tree growth across 10 temperate species on a productive forest site. Forest Ecol Manag 306: 142-149.

Figure legends

Figure 1. (a) Total ring area (*RA*) for the last five years (after the drought of 2012) against distance from the stem apex (*Dap*). **(b)** Tracheid cell wall thickness (*CWT*) for the last five years (after the drought of 2012) against *Dap*. Dark blue circles and light blue diamonds are for non-declining and declining trees, respectively. **(c)** Tracheid hydraulic diameter (*Dh*) for the last five years (after the drought of 2012) against distance from the stem apex (*Dap*).

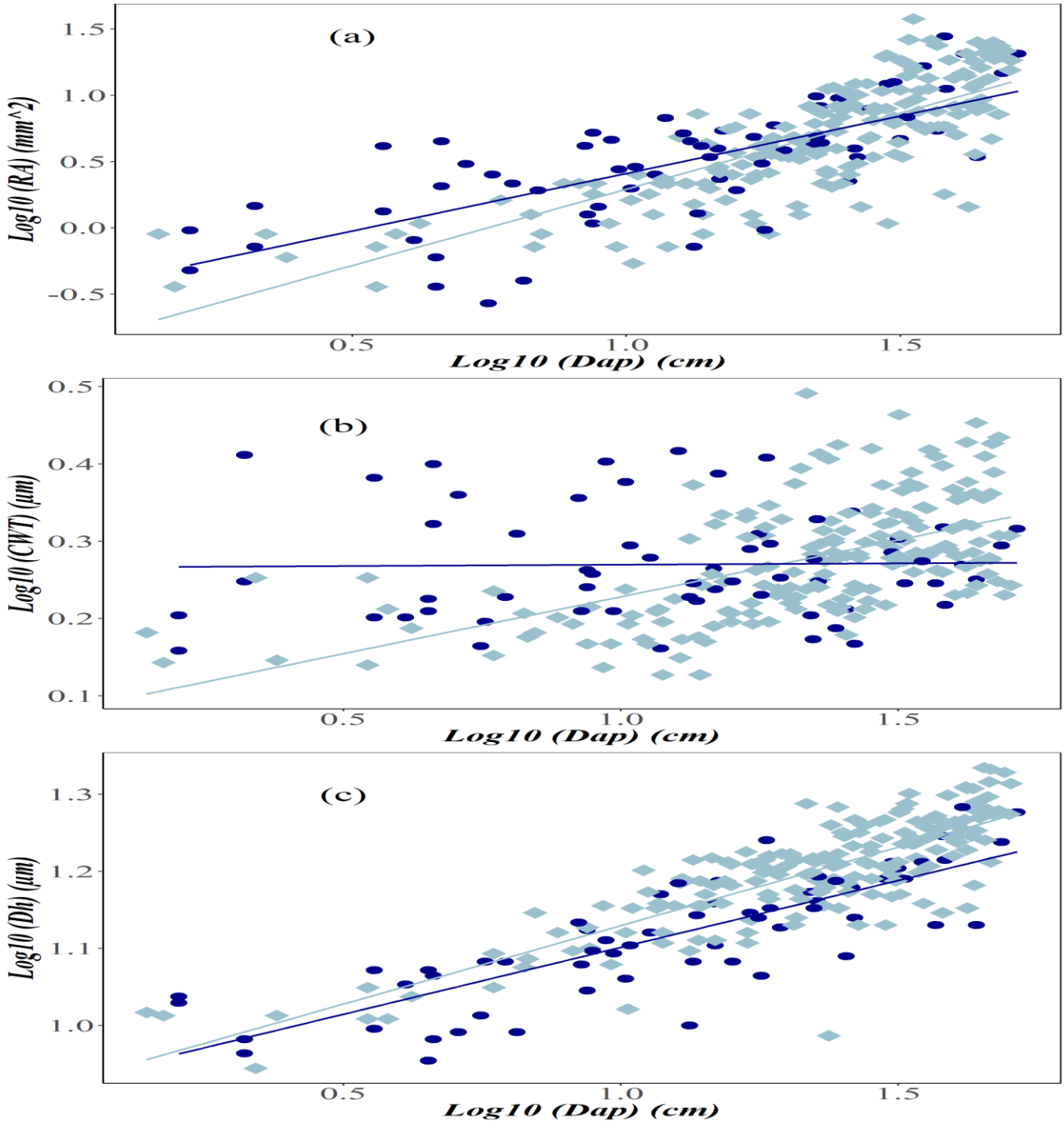

Figure 2. (a) Area of conductive phloem (*PAcond*) against distance from the stem apex (*Dap*). **(b)** Average diameter of the largest phloem sieve cells (*Dph*) for the last five years (after the drought of 2012) against *Dap*. Dark blue circles and light blue diamonds are for non-declining and declining trees, respectively.

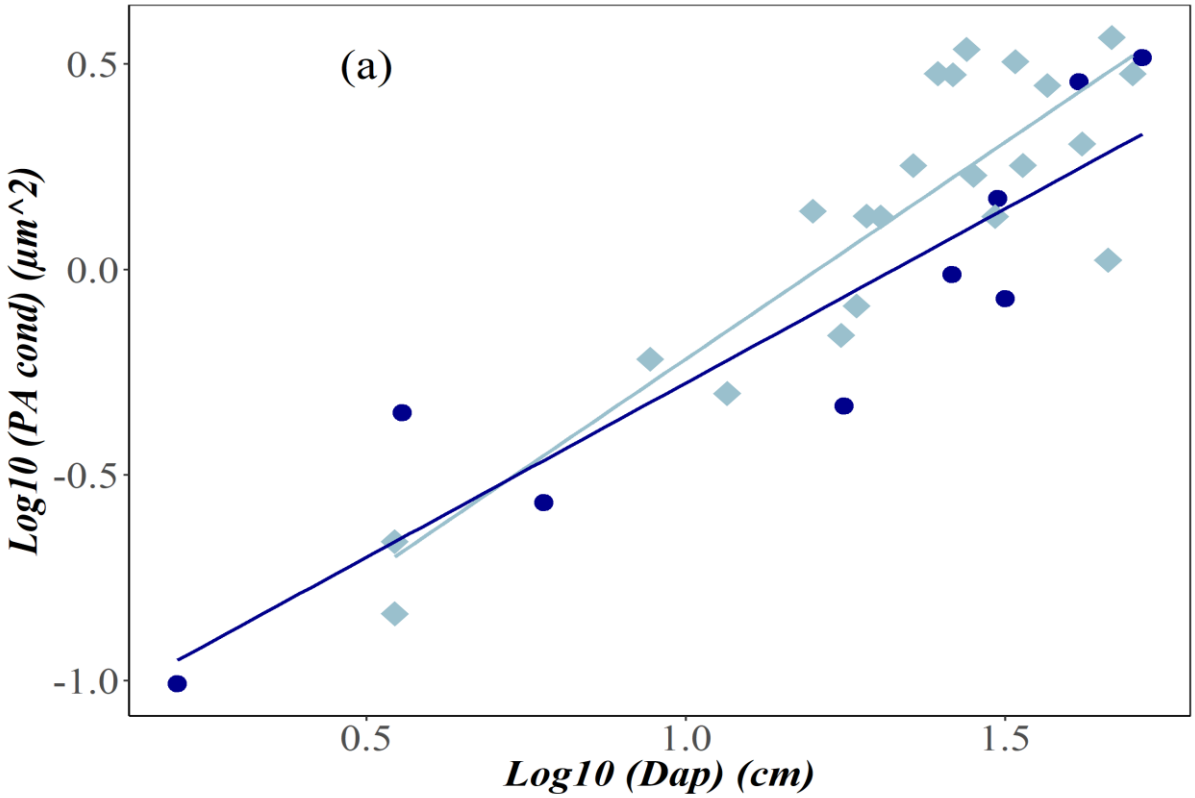

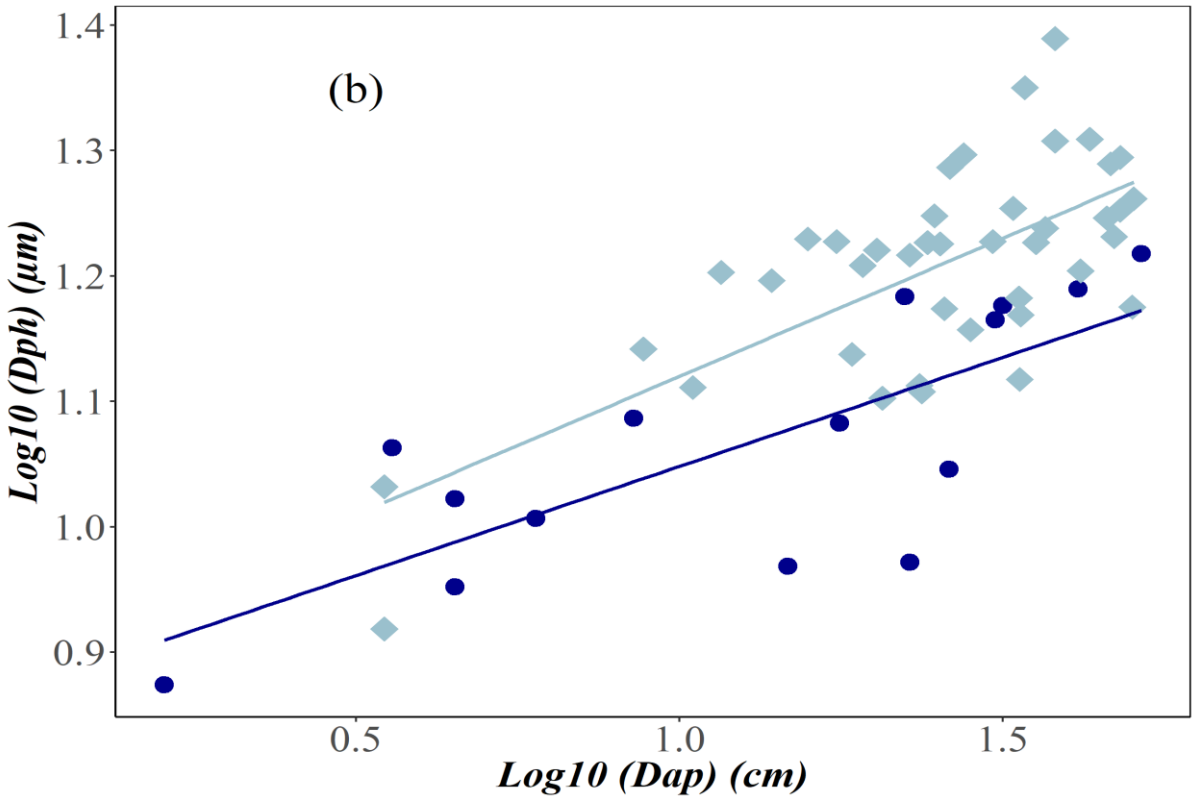

Table captions

Table 1. Diameter at breast height (*Dbh*), height (*H*), crown cover, age, and average stem elongation rate (*ΔH*) of the three declining and three non-declining sampled trees.

Table 2. Outputs of Standardized Major Axis (SMA) models. The models equal: *variable* ~ *Dap* + *conditions* to test for differences in elevation (y-intercept), and *variable* ~ *Dap*conditions* to test for differences in slopes (exponent *b*), where *Dap* is the distance from the stem apex (Warton et al. 2006, 2012). Data were log transformed. In the models variable = total ring area (*RA*) or tracheid cell wall thickness (*CWT*) or tracheid hydraulic diameter (*Dh*) or area of conductive phloem (*PAcond*) or average diameter of the largest phloem sieve cells (*Dph*), and conditions = declining and non-declining tree.

Table 2. Diameter at breast height (*Dbh*), height (*H*), crown cover, age and average elongation rate (*ΔH*) of the three declining and three non-declining sampled trees.

Condition	*Dbh* (cm)	*H* (m)	Crown cover (%)	Age (years)	*ΔH* (cm yr^{-1})
Declining	23.0	9.5	40	126	1.50
	21.3	10.7	20	115	2.94
	27.0	12.3	25	135	3.00
Non-declining	19.5	9.28	100	61	8.63
	21.0	10.5	90	90	3.04
	20.0	9.0	100	62	6.72

Table 2. Outputs of Standardized Major Axis (SMA) models. The models equal: *variable ~ Dap + conditions* to test for differences in elevation (y-intercept), and *variable ~ Dap*conditions* to test for differences in slopes (exponent *b*), where *Dap* is the distance from the stem apex (Warton et al. 2006, 2012). Data were log10 transformed. In the models variable = total ring area (*RA*) or tracheid cell wall thickness (*CWT*) or tracheid hydraulic diameter (*Dh*) or area of conductive phloem (*PAcond*) or average diameter of the largest phloem sieve cells (*Dph*), and conditions = declining and non-declining tree.

.

Model information		Intercept	Slope
Log10 RA vs Log10 Dap	*Declining*		
	Estimate	-1.199	1.480
	Lower limit	-1.357	1.350
	Upper limit	-1.042	1.623
	Non-declining		
	Estimate	-1.049	1.187
	Lower limit	-1.203	1.005
	Upper limit	-0.895	1.404
P-value		<0.01	0.02
Log10 CWT vs Log10 Dap	*Declining*		
	Estimate	-0.043	0.255
	Lower limit	-0.080	0.226
	Upper limit	-0.006	0.288
	Non-declining		
	Estimate	0.007	0.182
	Lower limit	-0.034	0.140
	Upper limit	0.049	0.235
P-value		<0.01	0.02
Log10 Dh vs Log10 Dap	*Declining*		
	Estimate	0.880	0.247
	Lower limit	0.856	0.227
	Upper limit	0.904	0.268
	Non-declining		
	Estimate	0.857	0.212
	Lower limit	0.834	0.183

	Upper limit	0.881	0.246
P-value		<0.01	>0.05
Log10 PA cond vs	*Declining*		
Log10 Dap	Estimate	-1.331	1.197
	Lower limit	-1.615	0.962
	Upper limit	-1.048	1.489
	Non-declining		
	Estimate	-1.418	0.926
	Lower limit	-1.755	0.651
	Upper limit	-1.080	1.318
P-value		>0.05	>0.05
Log10 Dph vs Log10	*Declining*		
Dap	Estimate	0.807	0.315
	Lower limit	0.725	0.250
	Upper limit	0.889	0.396
	Non-declining		
	Estimate	0.749	0.229
	Lower limit	0.666	0.157
	Upper limit	0.832	0.335
P-value		<0.05	>0.05